International Journal of Environment and Geoinformatics 10(4):064-076 (2023)

Research Article

Flood Impact Assessment in Koton Karfe Using Sentinel-1 Synthetic Aperture Radar (SAR) Data

Isiaka Ibrahim Opeyemi[1] Ajadi Sodiq Abayomi[2], Arowolo Sodiq Ayobami[1], Mustapha Suebat Oluwakemi[3], Kingsley Odinakachukwu Ndukwe[1], Oluoma Christian Chibuike[4]

[1] Department of Surveying and Geoinformatics, Federal University of Technology, Akure, Nigeria
[2] Itech Energy Company, Portharcourt, Nigeria
[3] Department of Fisheries & Aquaculture, School of Agriculture & Agricultural Technology, Federal University of Technology, Akure, Nigeria
[4] Department of Geoinformatics and Surveying, University of Nigeria, Nsukka, Nigeria

* Corresponding author: I. O. Isiaka
E-mail: isiakaibroheem@gmail.com

Received: 23.08.2023
Accepted 01.12.2023

How to cite: Isiaka et al., (2023). Flood Impact Assessment In Koton Karfe Using Sentinel-1 Synthetic Aperture Radar (Sar) Data, *International Journal of Environment and Geoinformatics (IJEGEO)*, 10(4): 064-076. doi.10.30897/ijegeo.1348753

Abstract

Flood has proven to be an incessant menace in Nigeria more threatening to riverine areas. The most recent flood ensued in 2022 as a result of heavy rainfall and the release of water from Lagdo Dam in Cameroon which became very devastating in many areas notably the Koton Karfe area in Kogi State, causing business shutdowns and the loss of lives and properties. In this work, Sentinel-1 Synthetic Aperture Radar (SAR) imagery was used for flood inundation mapping, and the accompanying damages were investigated using Landsat derived Land cover maps of Koton Karfe during the 2022 devastating flood. Overall, the results obtained in this study show that the regions that felt the impact of the flood the most were the southern and western areas, which must have experienced such an impact due to their proximity to the rivers Niger and Benue and also the water coming from the upper stream part of Cameroon. Further findings revealed that during the flood period on October 13, 2022, the total inundated area in Koton Karfe was estimated to be 198.255 sq. km. In terms of damage assessment, the urban areas had reduced from 220.902 sq. km in May 2022 to 87.473 sq. km in November 2022. This shows that over 133 sq. km of the urban settlement have been lost, indicating that lives must have been lost, properties too, and humans must have been displaced. This research will assist in the space of flood emergency response and disaster management.

Keywords: Flood, Sentinel-1, Synthetic Aperture Radar, Damage assessment, Koton Karfe, Disaster management

Introduction

Climate change is rapidly contributing to more threats and also emasculating human security and livelihoods of less adaptive and vulnerable communities in Africa and other parts of the world. Climate change can be an accelerant of instability that could exacerbate human security and undermine the livelihoods of vulnerable communities in fragile regions and hotspots where poverty, social insecurity, terrorism, and forced displacement are rampant (Scheffran et al., 2019).

According to a report by United Nations Office for Disaster Risk Reduction, it was reported that floods account for more than 40% of all the globally recorded disasters which took place between 1998 and 2017 (Nguyen et al., 2023). Although flood occurrence is difficult to prevent, predicting these catastrophic events requires appropriate methods and analysis (Cloke and Pappenberger 2009; Farina et al., 2018; Isiaka et al., 2023; Mentes et al., 2019; Moazzam et al., 2018; Ozulu et al., 2021). The occurrence of floods can result in threats of changes that can influence the temporal and spatial configuration of human life, loss of property, as well as having effects on agriculture and the environment. The incidence of flooding has risen tremendously which calls for an effective and comprehensive analysis of flood impacts to enable an informed response and alleviate the catastrophic consequence (Mohammad et al., 2014). The spatial and temporal patterns of disaster can be influenced by human activities in developing countries, including the rapid growth of unplanned residential areas, major land-use changes, and uncontrolled construction of buildings. In developing countries, many factors are responsible for flooding problems ranging from topography, poverty, land-use practice, urbanization, poor infrastructure, and climate change.

The devastating impacts of flooding have been experienced for many years and continue to affect people's lives and livelihoods, resulting in huge economic losses and social disruption (Mohammad et al., 2014). According to (Gebeyehu 1989), flood is the most common natural disaster that undermines human lives and the surrounding environment. The occurrence of flooding is most pronounced in Asia and African countries followed by Europe and the Americas. Specific countries may have varying levels of flood occurrence due to their geography and climate. In Kerala, India, heavy rainfall during the southwest monsoon season has led to disastrous flooding. In the year 2018, about 445 people were reported dead, and 14 missing cases. However, in 2019, the situation

worsened, with 121 casualties and 59 missing cases filed (Vishnu et al., 2019). In 2022, Nigeria experienced one of its worst flood disasters in recent occurrence. More than 26 of the 36 states including the Federal Capital Territory (F.C.T) were affected by floods, resulting in the death of hundreds of citizens and the destruction of houses. Also, expansive hectares of farmlands were ransacked, and roads and bridges were washed off leading to travelers sleeping on the roads for many weeks. Koton Karfe, a local government area (LGA) located in Kogi State, Nigeria, is one of the areas that experienced several devastating floods in recent years, which have affected the livelihoods of its residents.

To find lasting solutions to these challenges, there is an increasing demand for real-time observation and the implementation of advanced technologies to enable accurate mapping of flood-inundated areas. According to (Dumitru et al., 2014), it was suggested that the rapid estimation of the spatial scope of floods over extensive regions provides essential datasets for evaluating risk and spatial planning purposes. After carrying out an in-depth review of the existing literatures in the area of interest, it was observed that a significant dearth of studies specifically addressed the subject matter in Korton Karfe. The research gap allowed us to explore innovative approaches to fill the void and further develop the understanding of flood impact assessments in the area. In this research, we integrate Synthetic Aperture Radar (SAR) to evaluate the impact of floods. To our understanding, this is the first attempt to utilize SAR in assessing flood impacts in the Korton Karfe area of Kogi State, Nigeria. Highlighted by (Twele et al., 2016) is that optical remote sensing has been used for dynamic flood observation based on the high reflectance in the blue/green bands and low reflectance of water in the infrared region of the electromagnetic spectrum. During severe weather conditions as a result of heavy rainfall with a rugged dark cloud cover in flood-affected regions, optical remote sensing is not suitable for attaining precise results. Unlike optical data, which is strongly influenced by weather, spaceborne Synthetic Aperture Radar (SAR) data is particularly appealing in disaster monitoring (Li et al., 2018). Synthetic Aperture Radar (SAR) has been identified as a very promising approach for accurate and near real-time flood monitoring (Bangira et al., 2021; Carreño et al., 2019; Perrou et al., 2018; Qiu et al., 2021). The privilege it has in penetrating any type of cloud contributes to its effective operation in any weather conditions. Similarly, Mason et al. (2012) opined that SAR actively emits electromagnetic waves that are uninterrupted by weather conditions, day or night time, this gives SAR a higher penetration rate through various medium and effectively identify flood occurrences both in vegetated and urban areas. To carry out a flood impact assessment in the Koton Karfe, this study utilizes Synthetic Aperture Radar (SAR) remote sensing techniques, and damage assessment was carried out using the land cover maps of the area before and after the flood period. The present research work has the objectives to understand the concept of microwave remote sensing and its application in flood management over the study area, estimate the damages caused by flood and create a flood extent map of the area from the sentinel-1 image and land cover classification map from Landsat imagery before and after the flood event. By doing so, we hope to provide a better understanding of the severity by delineating the extent of the damage caused by the flood on land cover classes.

Study Area

This study was carried out in Koton Karfe local government area (LGA) of Kogi state located between latitude 7° 40' 00" N- 8° 30' 00" N and longitude 6° 40' 00" E - 7° 00' 00" E (Fig. 1) sharing close border with Lokoja LGA, the capital of Kogi state with its East and West borders formed along the tributaries of the Benue and Niger river, respectively. The people of this area are best known for their agrarian practices which range from fish farming to crop planting owing to the very accommodating climate system in the area as well as hunting. The area is recognized to often experience bi-climate seasons; the dry season which spans from November to March and the wet season which begins from April to October. The area covers over 1500 sq. km with an average elevation between 19m and 400m above sea level.

River Niger and Benue flow through its boundary and form a confluence in the state capital, this proximity between Lokoja and Koton Karfe has made the area as vulnerable to flooding as the state capital in any case of increased water level in the two rivers (Oyedele et al., 2022). They have been concerns in the past as over 250 lives have been lost, many people displaced and a host of businesses lost as a result of the cumulative effect of the devastating flood events of 1994, 2004, 2010, 2012, 2017, 2018, 2019 and 2020 (Oyedele et al., 2022). Also, in the disturbing flood of 2018, several communities were affected in Koton Karfe LGA (Osayomi et al., 2022) which wreaked havoc and threatened fishing activities in the area thus, aggravating the unemployment and poverty level of the people. The most recent devastating flood happened in the latter days of September 2022 and the water did not recede until after October nonetheless leading to interruption of travels, business shutdown, and loss of lives and properties.

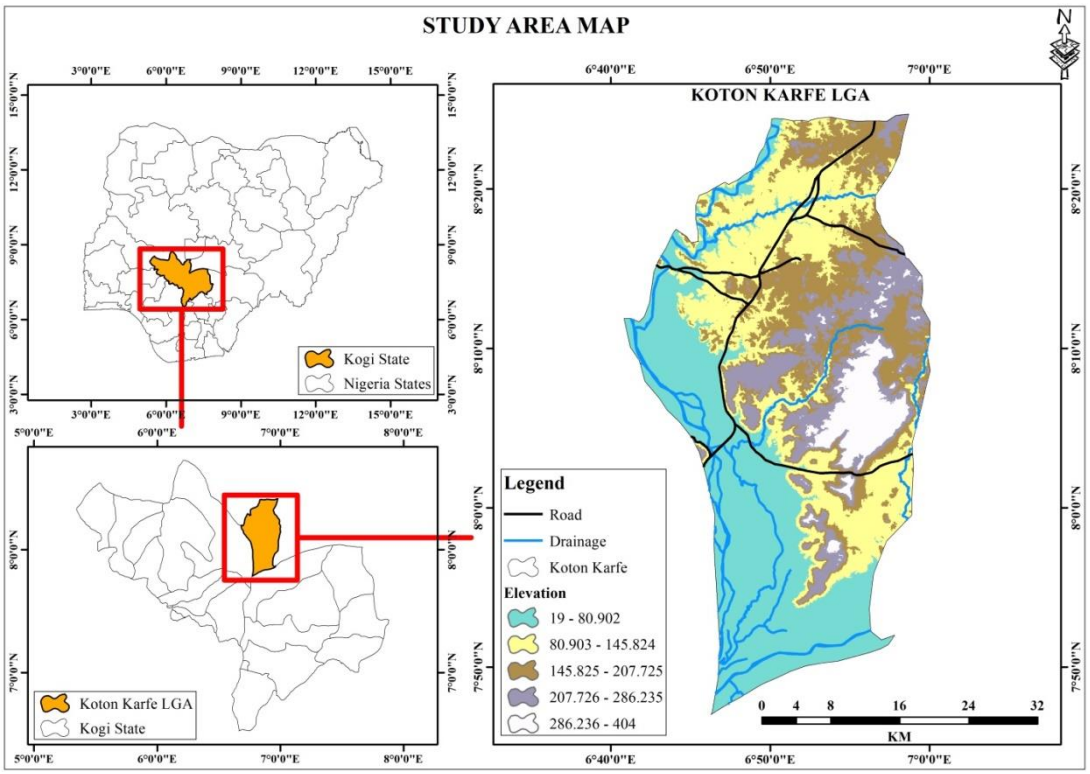

Fig. 1. Case Study Area of Research

Material and Methods

Data Sources

Sentinel-1 synthetic aperture radar (SAR) imagery was used to extract the flood extent map in this research. The sentinel-1 sensor was chosen because of its all-weather activeness and the short revisit time of 6 days between the two C- band equipped sentinel 1A and 1B satellites. The imagery can be acquired in different acquisition modes such as Strip map (SM), Extra wide swath (EW), Wave (WV), and Interferometric wide swath (IW). The data were acquired in IW acquisition mode as it default mode for land application (Benzougagh et al., 2021; Clement et al., 2018). The research is focused on extracting flood inundated areas thus data in the Ground Detected Radar (GRD) format and not the Single Look Complex (SLC) are acquired since the backscattering intensity information is the most required and not the additional phase information. Sentinel-1 imagery also has the advantage of providing free, well-timed data and was acquired from https://scihub.copernicus.eu/. Two Landsat imagery (one before the flood and another after the flood period) were acquired from https://earthexplorer.usgs.gov and used to ascertain the level of damage suffered from the flood. In further analysis of damage assessment, vector files of the villages and roads were integrated to determine the level of damage per community and road networks.

Sentinel-1 Data Preprocessing

The preprocessing steps identified in Fig. 2 were carried out and achieved through the use of Sentinel Application Platform 9.0 (SNAP) Desktop software. SNAP is an open-source tool whose operation has been augmented by several contributors. The tool has proven to be very useful in the processing of Sentinel-1 imagery and flood extent delineation using Sentinel-1 data. In the respect that this research covers Koton Karfe LGA, all the analysis on both Sentinel-1 and Landsat imagery had to be restricted to this area of interest. Three Sentinel-1 images have been processed for the flood extent mapping; one as achieve data and the other two as the crisis data taken during the flood period. The Sentinel-1 data are based on C-band synthetic aperture radar (SAR) and are best known not only for their all-weather capabilities but also for their strength in distinguishing land surface from water. Additionally, they have the edge of being cloud free over optical satellite data. The data also have a shorter revisit time compared to optical satellite imagery, a very useful characteristic in disaster management**.** In this research, the VV polarization was used and maintained for all three acquired SAR data, even though many researchers have adjudged SAR data with HH polarization best for flood detection (Henry et al., 2006; Psomiadis 2016) but so many other researchers have also considered using VV polarization for flood detection which also performed satisfactorily well (Twele et al., 2016; Ganji et al., 2019).

All the Sentinel-1 imagery acquired for this work had to be reduced to only cover the area of interest i.e. Koton Karfe LGA. This was achieved by creating a rectangle that will cover the area of interest on the sentinel imagery and the coordinates of the four corners of this rectangle were used to set the extent of the subset data. Reducing the size of the Sentinel-1 data does not compromise the data quality but only reduces the processing run time. The next preprocessing step is applying the orbit file. The SNAP automatically

downloads the updated orbit file as the initial orbit file gotten after acquiring the imagery from the Copernicus hub is incorrect but is updated online after a few days of image release thus, updating the metadata of the Sentinel-1 data and orient the data in the appropriate satellite position.

Table 1. Dataset

Acquisition Date	Flood Condition	Satellite/Source	Spatial Resolution/Pixel Spacing	Pass	Polarization
26/08/2022	Pre flood	Sentinel-1	20x22m/ 10x10m	Descending	vv
13/10/2022	During flood	Sentinel-1	20x22m/ 10x10m	Descending	vv
25/10/2022	During flood	Sentinel-1	20x22m/ 10x10m	Descending	vv
03/05/2022	Pre flood	Landsat	30m	-	-
19/11/2022	Post flood	Landsat	30m	-	-
-	Road and Village shapefiles	OSM	-	-	-

Removal of thermal noise is the next SAR preprocessing step. The Sentinel-1 imagery is accustomed to the surrounding noise of the SAR receiver which can be reduced by normalizing the backscatter signal of the Sentinel-1 imagery using the Thermal Noise Removal Command on SNAP (Benzougagh et al., 2021). The next step is applying the radiometric calibration operation which converts the Sentinel-1 image data into meaningful physical radar backscatter digital numbers from which the water and non-water objects on the Sentinel-1 imagery can be distinguished. Here, only the sigma naught (σ^0) was checked to be the output of the processing. Sentinel-1 imagery is often characterized by granular noise which is removed by applying the speckle filter command. This operation is as significant as the other steps in that if the granular noises are not removed the Sentinel-1 image could be wrongly interpreted. The single speckle filter was used with Lee Sigma as the filter, window size of 7 by 7 and sigma of 0.9 were also chosen. Lee filter was preferred because it makes the least compromises on the radiometric and spatial resolution of the Sentinel-1 data (Alvan et al., 2020). On adding the SAR data to SNAP, the imagery was inverted and not in its correct reference frame. Terrain correction was applied to fill this gap so that the imagery will be in sync with how they are projected in reality. Shuttle Radar Topography Mission (SRTM) DEM imagery of 3 arc-second with bilinear interpolation technique (used for resampling the image and Digital Elevation Model, DEM) and coordinate system set as (UTM/WGS1984 Geographic Projection) were used to run the terrain correction command which also addressed the errors due to terrain height. The final preprocessing step is the conversion of the radiometric pixel values of the resulting imagery from linear values to decibels (dB) which follows the equation (1).

$$\sigma^0_{dB} = 10 \log_{10} \sigma^0 \quad \text{(Eq.1)}$$

Where: σ^0_{dB} is backscatter image in dB and σ^0 is the output of preprocessed image

To optimize all the processing run time and for computerization, the entire preprocessing steps were put together and integrated using the graph builder tool, and the batch processing command was used to run the whole preprocessing workflow (Fig. 2).

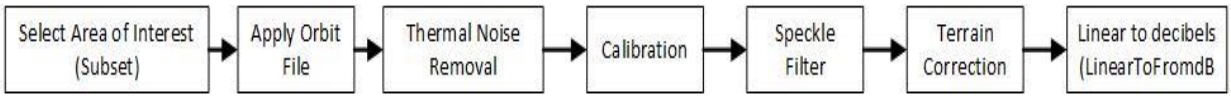

Fig. 2. The Methodological Workflow of the Sentinel-1 SAR Image Preprocessing

Sentinel-1 Image Processing

They are different methods of mapping flood water using SAR Sentinel-1 imagery which include; the binarization technique which uses a threshold value to detect the flood water; the change detection method by determining the ratio between SAR imagery before the flood and imagery after the flood and last is the use of RGB clustering technique. In this paper, the threshold technique was used to delineate flooded areas in Koton Karfe LGA. This technique requires the determination of a threshold value that distinguishes the water from non-water features.

It is worth noting that the dB image distinguishes water features from non-water features by showing them in dark color i.e. they have low backscatter value in most cases they are the negative values and hence are always in the darkest shades whereas the non-water features are mostly dry and rough on the surface thus have high backscatter values and are the bright color features on the backscatter image in dB. Herein, the histogram of the transformed preprocessed Sentinel-1 imagery was

generated and several threshold values were tested. This was done by creating shapefiles that fall on the dark color features of the backscatter image in dB and the statistics of these shapefiles were analyzed to arrive at a correct choice of threshold. A threshold of -18 dB was the chosen threshold value to distinguish the water from non-water which also corresponds to the mean value of the backscatter of the overlaid shapefiles. The band math function was initiated and the expression "if sigma0_vv < -18 then 2 else NaN" run. This command creates a binary map where areas with backscatter values that agree with the expression are assigned the value 2 (with a color) while areas that do not agree with the expression are represented as NaN (with no color). This was done for all three Sentinel-1 SAR imagery. The resulting map was then exported in Geotiff format for further analysis. Pre-flood water bodies vectorized from Landsat images acquired before the flood period were classified to be perennial water bodies because there were no flood news reports at the time. The pre-flood water bodies were superimposed on top of the flood maps to separate the flood inundation area from permanent water bodies. Advance analysis on the flood impact assessment to determine the extent of flood and areas affected as well as other statistical analyses were carried out in ArcGIS Environment and Microsoft Excel.

Land Use and Land Cover Classification Processing

To achieve the aim of this paper, land use, and land cover maps were prepared for Koton Karfe LGA before the flood event and after the flood event. Landsat-8 and Landsat-9 imagery that corresponds to the 03/May/2022 and 19/Nov/2022 respectively were obtained. All the geoprocessing steps to produce the LULC maps were carried-out using ENVI 5.3 and ArcGIS 10.7.1. Firstly, it was necessary to acquire cloud-free optical imagery between the period before the flood and after the flood event as well as important to carryout atmospheric and radiometric correction. In this research, geometric, radiometric and atmospheric corrections were carried-out. To begin, image geometric rectification is a fundamental precondition that must be completed prior to using images in Geographic Information Systems (GIS). Second, radiometric correction seeks to eliminate radiometric inaccuracies or distortions, whereas geometric correction seeks to eliminate geometric distortion. Finally, atmospheric adjustment was utilized to eliminate the target, as well as absorbed or dispersed effects. Hence, these corrections were performed before further analysis of determining the damage extent per land cover class. The maximum likelihood supervised classification model in ENVI 5.3 was used to derive the land cover map for the pre and post-flooding periods because it is often the most used supervised classification which is based on the premise that the training data statistics in each band are normally distributed (Richards and Jia 2006). Although there are other sophisticated supervised classification techniques that have been used for land cover classification, such as neural networks and support vector machines (SVM), nevertheless researchers like Ali et al., (2018) employed maximum likelihood model in the land cover classification using Landsat imagery with a performance score of 91.34% and 0.89 as the overall accuracy score and Kappa coefficient, respectively. In a similar study of land cover mapping by Norovsuren et al., (2019) of Khandgait in Mongolia from 2000 to 2019, the model performed with over 80% overall accuracy. The maximum likelihood model have also been employed by Akinyemi (2005) to monitor land use patterns in the southwestern Nigeria and Ojigi (2006) also looked at various supervised classification techniques to monitor changes in the Abuja landscape. The results showed that the maximum likelihood algorithm performed better than other algorithms such as the minimum distance, parallelepiped, and fisher's classifications model. Thus, if data are obtained according to a normal distribution, the maximum likelihood model is still applicable and will continue to function properly. To facilitate this procedure and to achieve an accurate land cover map, Google Earth imagery of the area was acquired and used to aid in selecting and assigning different land cover classes to pixel values while developing the training samples for the model. The land cover map was classified into six land cover types (Urban, Water Bodies, Dense Vegetation, Less Dense Vegetation, Cropland, and Barren Land). Accuracy evaluation is one of the most crucial last steps in the classification process. The goal of accuracy evaluation is to quantify how well pixels were sampled into the correct land cover classes therefore; Sixty (60) random points were selected to determine the overall classification accuracy and its kappa coefficient of the LULC maps. The land cover maps derived from ENVI were exported to ArcGIS Environment where the damage assessment and other statistical summaries were derived after the extraction of the perennial water bodies. The percentage change (i.e. the loss or gain) for the land covers was computed from equation (2):

$$\%\ Change = \left(\frac{A_{PTF} - A_{PRF}}{A_{PRF}}\right) * 100\% \qquad \text{(Eq.2)}$$

Where: A_{PRF} is the area covered in the Pre-Flood LULC Map and A_{PTF} is the area covered in the Post-Flood LULC Map.

Result and Discussion
Flood Inundation Mapping

The need to develop a SAR remote sensing technique for flood damage assessment in Koton Karfe is a significant and valuable approach because the area has been experiencing recurring flooding, which has always led to severe environmental and socio-economic losses.

The flood inundation map (Fig. 3) describes the progression and recession of the devastating flood of 2022 in the Koton-Karfe region of Kogi State, Nigeria delineated from the Sentinel-1 SAR imagery. The applications of SAR data have been identified to be more effective and accurate for delineating flood inundation. Flood-inundated areas extracted from Sentinel-1 imagery of October 13, 2022, are shown in

orange while those from October 25, 2022, are shown in grey colors (Fig. 3). The water bodies extracted from the acquired Sentinel-1 imagery of August 26, 2022, represent the perennial water bodies (i.e. rivers) in Koton Karfe as the flood had not begun until the latter part of September. The resulting inundation map shows that the regions that felt the impact of the flood the most were the Southern and Western areas, which must have experienced such due to the proximity to rivers Niger and Benue and also the water coming from the upper stream part of Cameroon.

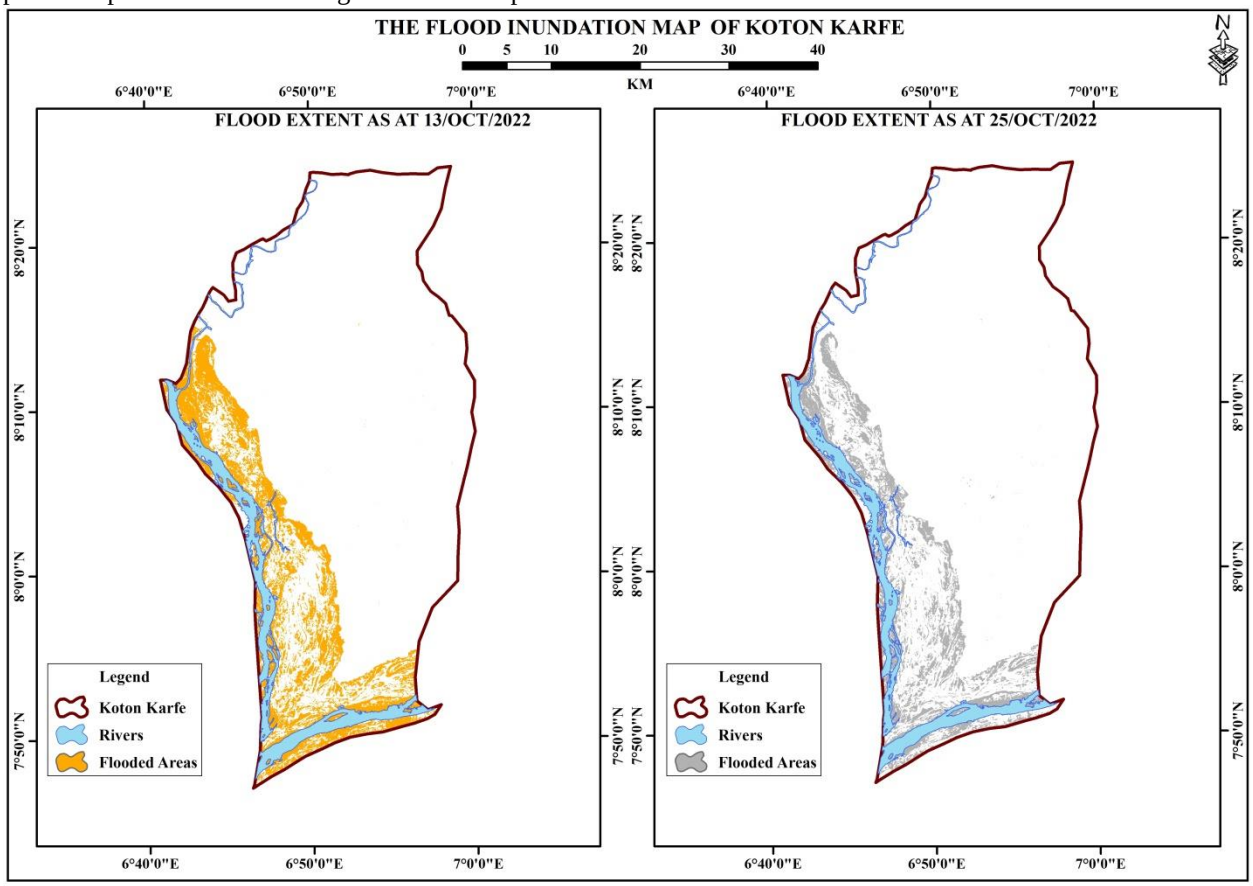

Fig. 3. Flood Inundation Map of Koton Karfe LGA.

The extracted water bodies from the Sentinel-1 imagery obtain for August 26th, 2022 represent the perennial water bodies and by removing its area covered from the total surface water covered by acquired data of the other dates, the inundated areas were ascertained. Before the flood had started, Koton Karfe had total permanent water covering 80.770 sq. km. In Nigeria and other West African countries, April to November marked the wet season. Moreover, heavy rainfall usually starts from early September to the middle of November. Severe rainfall that started in early September together with the release of water from the Lagdo dam in Cameroon, on the 13th of September 2022 contributes to this flooding in the area.

The finding of this research shows that during the flood period, on October 13th, 2022, the total inundated area in Koton Karfe was estimated to be 198.255 sq. km. Further findings indicate that the water level on the 25th of October, 2022 had only receded by ~54.00 sq. km leaving the estimated inundated area at 144.250 sq. km. This could be a result of the area receiving less intense rainfall and/or the water coming from the Lagdo dam and upstream dams in Nigeria to have spread to the downstream part of the country. In the research conducted by (Mata et al., 2022), it was pointed out that spatial variability of flood extent can be attributed directly to several factors such as precipitation, land cover types, and topographic conditions. Results also showed that maximum flood inundation occurred during mid of October submerged ~200 sq. km area of the region and that there is about 3 times increase in the volume of the perennial water bodies in Koton Karfe (Fig. 4). Many research studies have highlighted the suitability of Sentinel-1 (SAR) in accurately mapping flood-affected regions, largely because of its ability to penetrate through cloud cover. The finding from the present study align with and support the conclusions of earlier research conducted by (Moharrami et al., 2021), which employed multi-temporal Sentinel 1 images to monitor flood events.

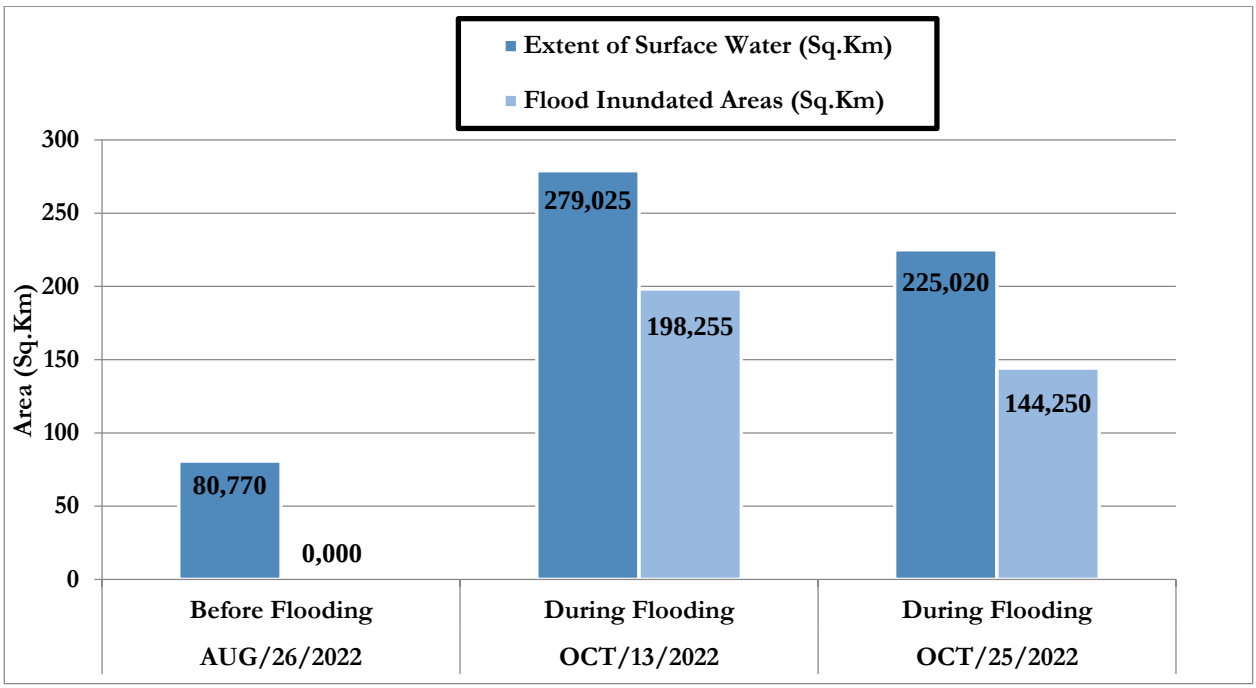

Fig. 4. Area Covered by Flood Water

Damage Assessment Analysis

The study aim to find the impact of the 2022 flood in Koton Karfe and it found that the flood had a widespread impact on Koton Karfe, affecting a variety of land use and land cover categories such as the urban areas, water bodies, dense vegetation, less dense vegetation, barren land, and croplands. The examination of the LULC maps both before and post the flood offered valuable insights into the magnitude of the flood damage in the study area. The flood damage has been assessed from the derived pre-flooding and post-flooding land use and land cover map (Fig. 5).

Very noteworthy from Fig. 5 is the emphasis on the black circle which covers a sampled area in Koton Karfe showing the land cover before and after the flood event. The result shows that the area covered by the circle was initially characterized majorly by vegetation (Dense, less dense, and cropland) but five months later after the flood the same area has seen its land cover classes change to predominantly barren land and some little area of dense vegetation. The trend of these changes can be noticed throughout the land cover maps below.

The data extracted from Landsat developed a technique for assessing the accompanying losses accrued as a result of the flood is shown in Table 2. The LULC classification accuracy and kappa coefficient of the pre-flood map are 93.02% and 0.92, respectively while the overall accuracy for the post-flooding map is 94.25% and its kappa coefficient is 0.93. It became necessary to determine these accuracy values before any further analysis can be extracted from the LULC maps and herein, the values gotten are satiable. The trend of the land cover classes shows that between May 2022 and November 2022 which corresponds to the pre-flood and post-flood periods, respectively, the urban areas had reduced from 220.902 sq. km to 87.473 sq. km. This shows that over 133 sq. km of urban settlement have been lost which invariably means some lives were lost, properties lost and humans must have been displaced. The water bodies trends show that from 68.537 sq. km in May 2022 they have risen to 108.893 sq. km by the end of the flood period in November 2022. This excludes the perennial water bodies in Koton Karfe but rather the new and artificially created lakes and wetlands.

The aftermath of the flood saw an increase amounting to 40.356 sq. km of water bodies in Koton Karfe which must have influenced the urban settlement lost and some vegetation where the only green that can withstand such submerge is the dense vegetation (forest). This trend is seen as the densely vegetated areas increased by 273.613 sq. km which is understandable as these areas are mostly forest zones with thick trees that will withstand such sink. However, the cropland area also increased from 195.831 sq. km before the flood to 482.252 sq. km after the flood but this is most likely unwanted plants (weeds) because this much water will destroy the crops by either altering the areas to barren lands or increased the numbers of crop plants but with zero production from the crops (i.e. weeds). The former can be seen in the case of less dense vegetation as they have been reduced to 277.522 sq. km from 516.137 sq. km. During flooding the most vulnerable land cover are the bare/barren lands. The barren lands in Koton Karfe lost 91.747 sq. km from its initial 317.994 sq. km. All this data will be very pertinent in immediate damage response and in managing the flood disaster as they contain pointers to the areas that are most affected and the areas that saw improvements.

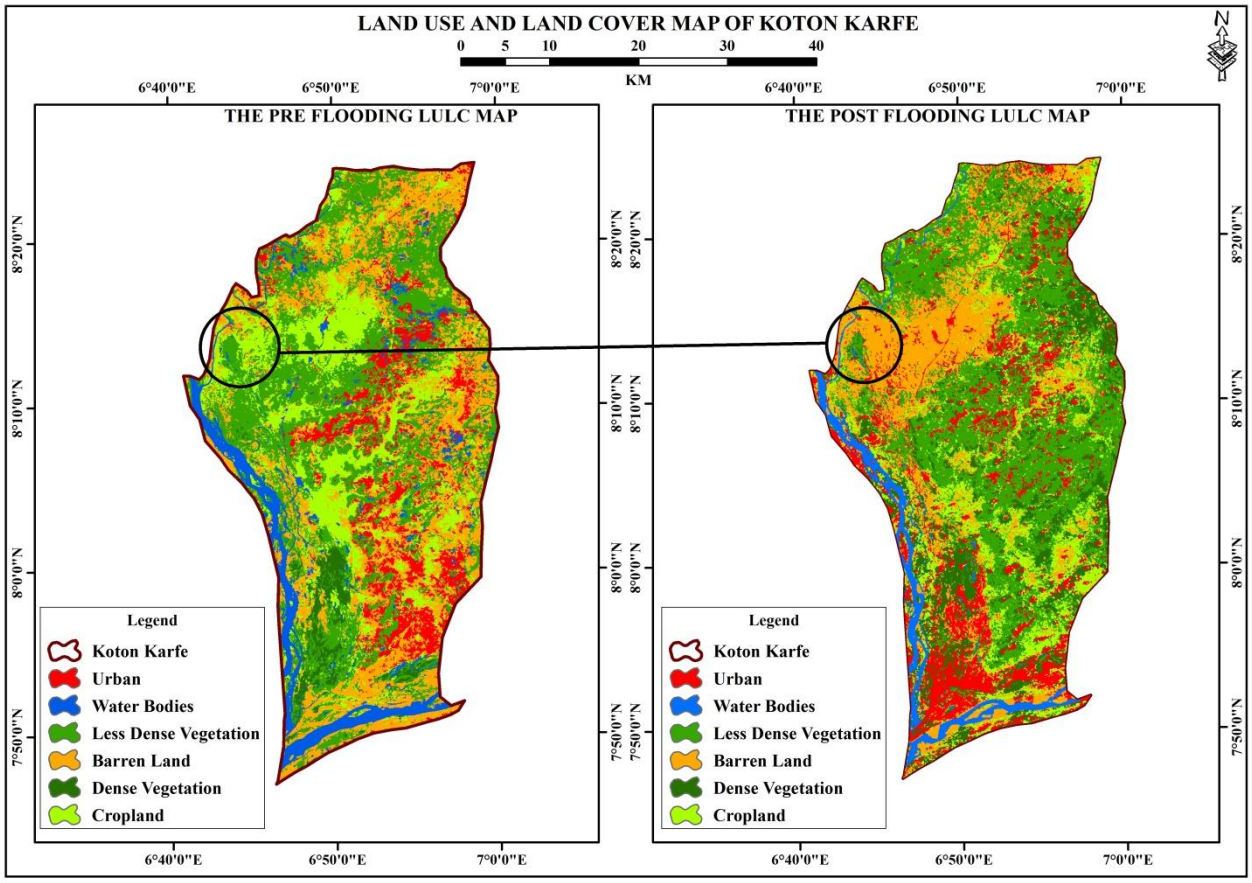

Fig. 5. Pre and post flooding LULC maps showing affected areas especially loss of croplands

Table 2. Land use land cover analysis

	MAY AREA (Sq.Km)	NOV AREA (Sq.Km)	DIFFERENCE (Loss/Gain)
Urban	220.902	87.473	-133.430
Water Bodies	68.537	108.893	40.356
Less Dense Vegetation	516.137	277.522	-238.615
Barren Land	317.994	226.247	-91.747
Dense Vegetation	208.639	482.252	273.613
Cropland	195.831	345.654	149.823
Overall Accuracy	93.02%	94.25%	
Kappa Coefficient	0.9162	0.9305	

Fig. 6 provides insight into the percentage change in land use and land cover resulting from the flood and these findings are consistent with the results of Table 3 and provide further results as to how the land cover classes have increased from the initial extent before the flood. The cropland saw an increase of 76.51% of the initial areas cover before the flood period. The dense vegetation gained twice the area it covered before the flood period. This shows the level of water present in this area. Equally these areas are also characterized by wetlands where small ponds and rice farms are situated. Any flood occurrence will be accompanied by an increased water body and the result from this research shows that the water bodies in the area increased by 58.88% of the initial water bodies. Barren land, less dense vegetation, and urban settlements resulted in the loss of 28.85%, 46.23%, and 60.40%, respectively.

In totality (Fig. 6) highlights the significant percentage gain in dense vegetation and cropland and the significant percentage loss of urban areas, less dense vegetation, and barren land. These findings provide further evidence of the impact of the flood on land cover classes and show that the ecological balance of the affected area has been significantly altered. The loss of urban areas can have severe socio-economic impacts, including damage to infrastructure, loss of livelihoods, and displacement of people. In this study, the loss of urban areas may have led to severe economic losses, particularly for small and medium enterprises located very close to the river Niger and Benue banks. The loss of less dense vegetation and barren land can have significant environmental impacts, including soil erosion, loss of biodiversity, and reduction in the capacity to support agriculture. These impacts can have long-term consequences on the environment and the economy of the area and the state.

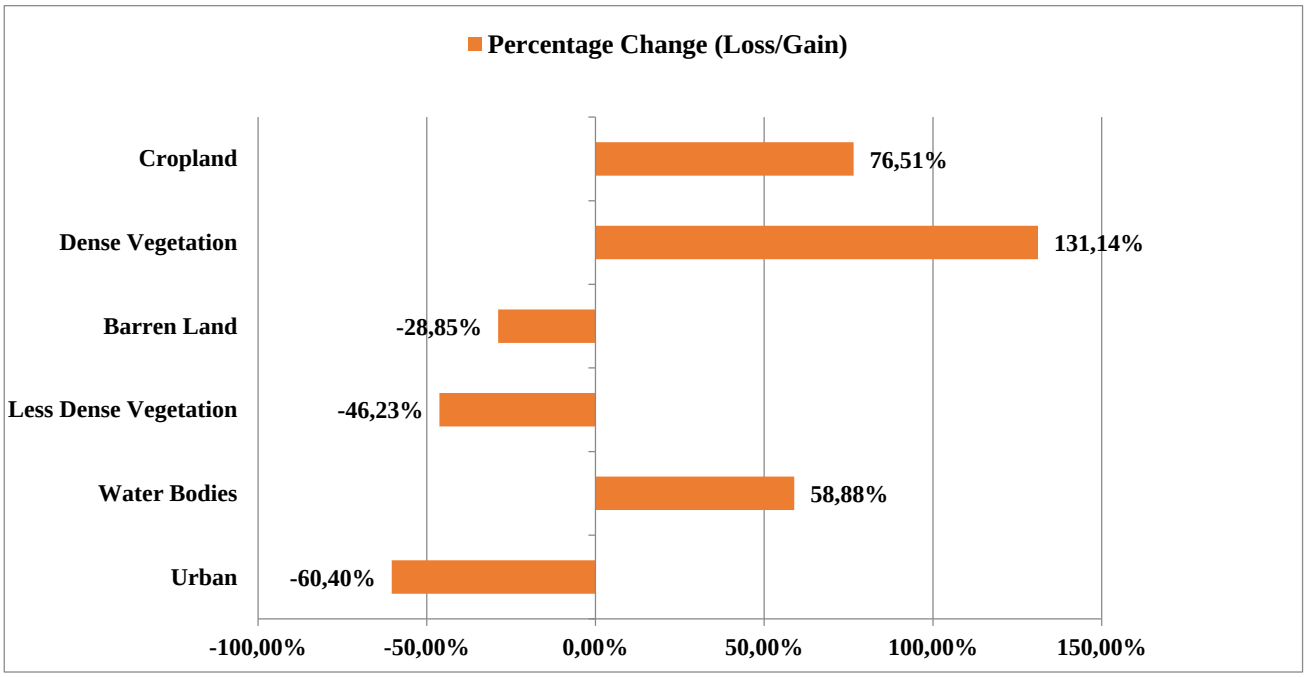

Fig. 6. Percent Change of Land Cover Classes

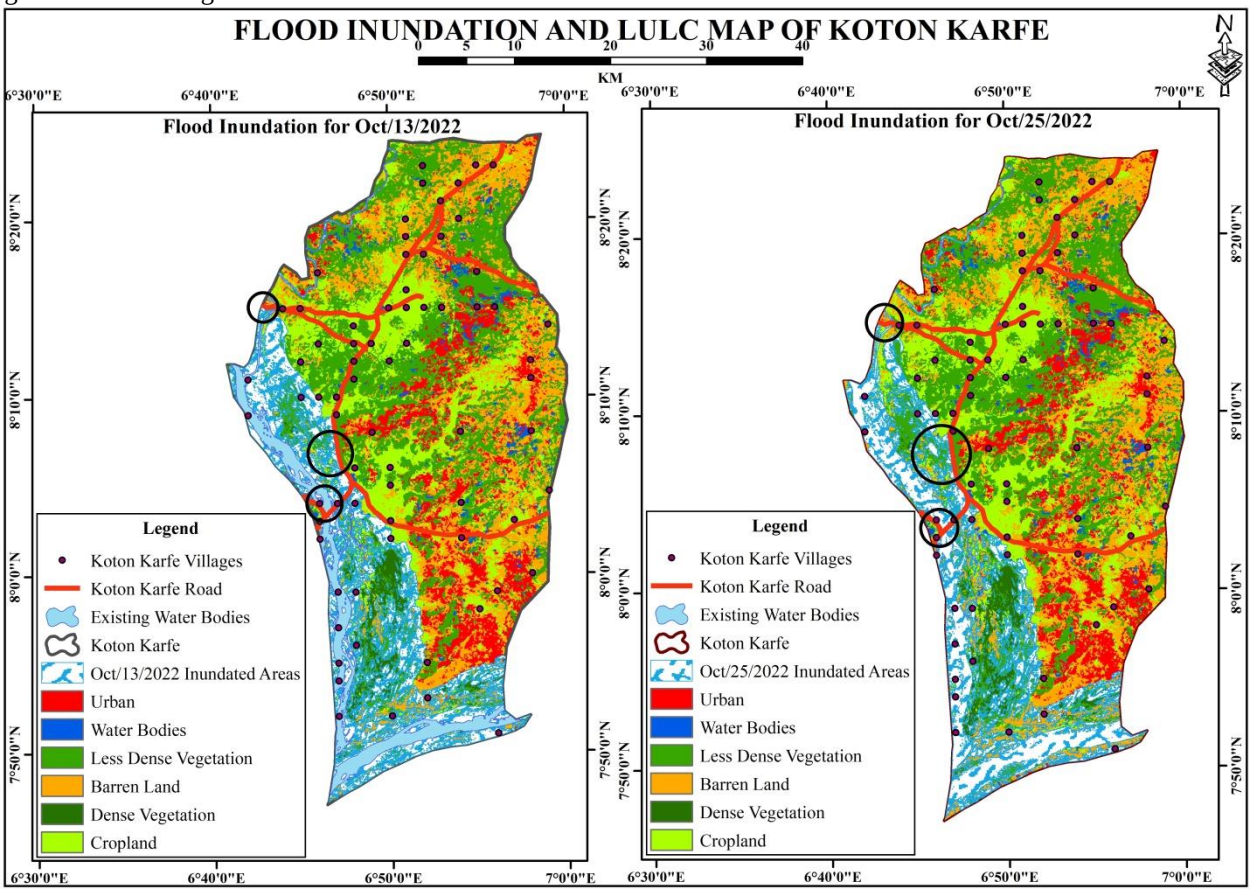

Fig. 7. Final inundation map of the Koton Karfe

The final inundation map of the Koton Karfe is shown in Fig. 7. The two tiles indicate the flood inundated areas on October 13, 2022, and October 25, 2022. The figure shows a flood-inundated map superimposed on the land cover map and the vector files of the roads as well as the villages in Koton Karfe. Further analysis from the flood inundation maps confirms that three different sections of the road (Three black circles) have been cut off by the flood water very notable is the bridge flying over River Niger (First circle from below) also known as the Jamata Bridge. This knowledge if integrated with the mass media could be leveraged by making a broadcast nationwide about the extent of the damage that has been caused on the road to possible commuters as this route is the popular route that connects the Northern part of Nigeria to its Southern part. It is also a major route for

transporting farm produces and other goods to and fro the northern and southern geopolitical zones of the country. This information will also be very useful to the humanitarian department and the emergency response team in appropriately managing the situation. Twelve days after the first inundation map show a very little decline from the initial water level noticed on 13 October 2022. Also, a total of twenty (20) villages were submerged during the two instances of the overlaid flood inundated map. This is another very important input in disaster monitoring indicators.

Conclusion

Sentinel-1 SAR is a microwave remote sensing technique that has proven to be very effective in flood inundation mapping as well as in flood disaster monitoring because of its all-weather capability, night/day time data capturing, freely available data, and high strength to distinguish between water and land. This research integrates Sentinel-1 spaceborne SAR imagery and Landsat-derived land cover maps to delineate flood-inundated areas and the accompanied damage incurred in Koton Karfe LGA Kogi State during the devastating flood of 2022. In summary, we have demonstrated the usage of Sentinel-1 imagery to extract the flood-inundated areas by first, removing the perennial water bodies from the derived flood maps, and with the integration of land cover maps the land cover classification that has experience damages were identified. Also, the road infrastructures and the communities in this area were overlaid on the flood inundation maps to identify the impact of the flood on them. The resulting land cover maps were classified into urban areas, less dense vegetation, dense vegetation, cropland, and barren lands with urban areas suffering the most losses during the flood incident. The result also shows that twenty communities and a major bridge, all characterized to be very close to the river Niger and Benue, were also submerged.

Based on our findings, this technique could be a very resourceful tool for assessing flood damage assessment in the hands of emergency response agencies and can be applied in other areas with similar floods happening. However, this could be improved by introducing cloud computing methods like using the Google Earth Engine because of the large data involved in this analysis. Overall, this research will be a very good addition to the field of environmental and flood management science.

This study has illustrated how very helpful the integration of Sentinel-1 spaceborne Synthetic Aperture Radar (SAR) resulting flood extent maps and Landsat-derived land cover maps can be in flood disaster management. In that respect, the following recommendations have been highlighted:

1. The approach presented in this study can be useful for preliminary planning for disaster response using freely available radar data and open-source software.
2. Development of a detailed flood risk map to identify the most vulnerable areas, thereby facilitating the implementation of effective mitigation and adaptation measures.
3. Government should enforce strict regulations to ensure that floodplain areas are used for compatible land uses that do not increase the risk of flooding
4. Land use planning, and proper construction practices to avoid building in high-risk areas should be given optimum attention.
5. This study's findings could be enhanced by performing crop type and fisheries type discrimination to assess the loss for specific types of crops and seafood products.
6. Finally, floods in some cases cannot be prevented but in such cases, adaptive measures should be developed by the authority's in-order to be able to withstand the changes that accompany this disaster.

Acknowledgements

We are appreciative to European Space Agency (ESA) for providing the sentinel-1 data through their website https://scihub.copernicus.eu/ also; they provided the SNAP 9.0 software https://eo4society.esa.int/resources/snap/ that was used to process the imagery. Landsat data used for this study, accessed through USGS Earth Explorer (https://earthexplorer.usgs.gov), SRTM data for this study area map was assessed through https://www.earthdata.nasa.gov/ as well as the vector data accessed via OpenStreetMap (https://www.openstreetmap.org/). In totality, we are grateful to all the organization that has made available all the dataset that were used for this research.

References

Akinyemi, F. O. (2005). Mapping land use dynamics at a regional scale in southwestern Nigeria.

Ali, M. Z., Qazi, W., Aslam, N. (2018). A comparative study of ALOS-2 PALSAR and landsat-8 imagery for land cover classification using maximum likelihood classifier. *The Egyptian Journal of Remote Sensing and Space Science*, 21, S29-S35.

Alvan Romero, N., Cigna, F., Tapete, D. (2020). ERS-1/2 and Sentinel-1 SAR data mining for flood hazard and risk assessment in Lima, Peru. *Applied Sciences*, 10(18), 6598.

Bangira, T., Iannini, L., Menenti, M., Van Niekerk, A., Vekerdy, Z. (2021). Flood extent mapping in the Caprivi floodplain using sentinel-1 time series. *IEEE Journal of selected topics in applied earth observations and remote sensing*, 14, 5667-5683.

Benzougagh, B., Frison, P. L., Meshram, S. G., Boudad, L., Dridri, A., Sadkaoui, D., ..., Khedher, K. M. (2021). Flood Mapping Using Multi-temporal Sentinel-1 SAR Images: A Case Study—Inaouene Watershed from Northeast of Morocco. *Iranian Journal of Science and Technology, Transactions of Civil Engineering*, 1-10.

Carreño Conde, F., De Mata Muñoz, M. (2019). Flood monitoring based on the study of Sentinel-1 SAR images: The Ebro River case study. *Water*, 11(12), 2454.

Clement, M. A., Kilsby, C. G., Moore, P. (2018). Multi-temporal synthetic aperture radar flood mapping using change detection. *Journal of Flood Risk Management*, 11(2), 152-168.

Cloke, H., Pappenberger, F. (2009). Ensemble flood forecasting: A review. *Journal of Hydrology*, 375(34), 613- 626.

Dumitru, C. O., Cui, S., Faur, D., Datcu, M. (2014). Data analytics for rapid mapping: Case study of a flooding event in Germany and the tsunami in Japan using very high resolution SAR images. *IEEE Journal of Selected Topics in Applied Earth Observations and Remote Sensing*, 8(1), 114-129.

Farina, G., Bernini, A., Alvisi, S., Franchini, M. (2018). Preliminary GIS elaborations to apply rapid flood spreading models. *EPiC Series in Engineering*, 3, 684-691.

Ganji, K., Gharachelou, S., Ahmadi, A. (2019). Urban's river flood analysing using Sentinel-1 data case study:(Gorganrood, Aq'qala). The International Archives of the Photogrammetry, Remote Sensing and Spatial Information Sciences, 42, 415-419.

Gebeyehu, A. (1989). Regional Flood Frequency Analysis. Hydraulics Laboratory, The Royal Institute of Technology, Stockholm. *Bulletin No. TRITA-AVI-148.*

Henry, J. B., Chastanet, P., Fellah, K., Desnos, Y. L. (2006). Envisat multi-polarized ASAR data for flood mapping. *International Journal of Remote Sensing*, 27(10), 1921-1929.

Isiaka, I. O., Gafar, S., Ajadi, S. A., Mukaila, I., Ndukwe, K. O., Mustapha, S. O. (2023). Flood Susceptibility Assessment of Lagos State, Nigeria using Geographical Information System (GIS)-based Frequency Ratio Model. *International Journal of Environment and Geoinformatics*, 10(1), 76-89.

Li, Y., Martinis, S., Plank, S., Ludwig, R. (2018). An automatic change detection approach for rapid flood mapping in Sentinel-1 SAR data. *International Journal Of Applied Earth Observation And Geoinformation*, 73, 123-135.

Mason, D. C., Schumann, G. P., Neal, J. C., Garcia-Pintado, J., Bates, P. D. (2012). Automatic near real-time selection of flood water levels from high resolution Synthetic Aperture Radar images for assimilation into hydraulic models: *A case study. Remote Sensing of Environment*, 124, 705-716.

Mata, C. B., Balderama, O. F., Alejo, L. A., Bareng, J. L. R., Kantoush, S. A. (2022). Satellite-based flood inundation and damage assessment.

Menteş, E. N., Şinasi, K. A. Y. A., Tanik, A., Gazioğlu, C. (2019). Calculation of flood risk index for Yesilirmak Basin-Turkey. *International Journal of Environment and Geoinformatics*, 6(3), 288-299.

Moazzam, M. F. U., Vansarochana, A., Rahman, A. U. (2018). Analysis of flood susceptibility and zonation for risk management using frequency ratio model in District Charsadda, Pakistan. *International Journal of Environment and Geoinformatics*, 5(2), 140-153.

Mohammad Muqtada Ali Khan., Nor Ashikin Shaari., Arham Muchtar Achmad Nahar., Md. Azizul Baten., Dony Adriansyah Nazaruddin. (2014). Flood impact assessment in Kota Bharu, Malaysia: a statistical analysis. World *Applied Sciences Journal*, 32(4), 626-634.

Moharrami, M., Javanbakht, M., Attarchi, S. (2021). Automatic flood detection using sentinel- 1 images on the google earth engine. *Environmental Monitoring and Assessment, 193*, 1-17.

Nguyen, T. H., Ricci, S., Piacentini, A., Fatras, C., Kettig, P., Blanchet, G., ..., Baillarin, S. (2023). Assimilation of SAR-derived flood extent observations for improving fluvial flood forecast–A proof-of-concept. *In IOP Conference Series: Earth and Environmental Science* (Vol. 1136, No. 1, p. 012018). IOP Publishing.

Norovsuren, B., Tseveen, B., Batomunkuev, V., Renchin, T., Natsagdorj, E., Yangiv, A., Mart, Z. (2019, November). Land cover classification using maximum likelihood method (2000 and 2019) at Khandgait valley in Mongolia. In IOP Conference Series: Earth and Environmental Science (Vol. 381, No. 1, p. 012054). IOP Publishing.

Ojigi, L. M. (2006). Analysis of spatial variations of Abuja land use and land cover from image classification algorithms. *In Symposium Remote Sensing: From Pixel to Processes*, Enschede, Netherlands (p. 6).

Osayomi, T., Jnr, P. O., Ogunwumi, T., Fatayo, O. C., Akpoterai, L. E., Mshelia, Z. H., Abatcha, I. U. (2022). "I lost all I had to the flood…": A Post-Disaster Assessment of the 2018 Kogi State Flood in Nigeria. *Ife Social Sciences Review*, 30(2), 1-20.

Oyedele, P., Kola, E., Olorunfemi, F., Walz, Y. (2022). Understanding flood vulnerability in local communities of Kogi State, Nigeria, using an index-based approach. *Water*, 14(17), 2746.

Ozulu, G., Essien, G. P., Akudo, E. O. (2021). Geological and Geospatial Mapping of Vulnerability Areas for Proper Flood Mitigation: Ganaja, Lokoja Metropolis, North-Central Nigeria. *International Journal of Environment and Geoinformatics*, 8(3), 267-275.

Perrou, T., Garioud, A., Parcharidis, I. (2018). Use of Sentinel-1 imagery for flood management in a reservoir-regulated river basin. *Frontiers of Earth Science*, 12, 506-520.

Psomiadis, E. (2016, October). Flash flood area mapping utilising SENTINEL-1 radar data. *In Earth resources and environmental remote sensing/GIS applications VII* (Vol. 10005, pp. 382-392). SPIE.

Qiu, J., Cao, B., Park, E., Yang, X., Zhang, W., Tarolli, P. (2021). Flood monitoring in rural areas of the Pearl River Basin (China) using Sentinel-1 SAR. *Remote Sensing*, 13(7), 1384.

Richards, J. A., Jia, X. (2006). Image classification methodologies. *Remote sensing digital image analysis: An introduction*, 295-332.

Scheffran, J., Link, P. M., Schilling, J. (2019). Climate and conflict in Africa. *In Oxford Research Encyclopedia of Climate Science.*

Twele, A., Cao, W., Plank, S., Martinis, S. (2016). Sentinel-1-based flood mapping: a fully automated processing chain. International Journal of Remote Sensing, 37(13), 2990-3004.

Vishnu, C. L., Sajinkumar, K. S., Oommen, T., Coffman, R. A., Thrivikramji, K. P., Rani, V. R., Keerthy, S. (2019). Satellite-based assessment of the August 2018 flood in parts of Kerala, India. Geomatics, *Natural Hazards and Risk,* 10(1), 758-767.